An MGI approach for discovering solid-state electrolytes materials for Li-ion battery

Introduction to solid-state electrolyte materials for Li-ion batteries:

Li-ion batteries have become an integral part of our modern lifestyles because of their ubiquity and versatility. These devices are the leading power source for mobile electronics like smartphones, laptops, cameras, e-readers, tablets, etc. because of their higher energy and power density as compared to the other energy storage technologies.[1] A typical Li-ion battery consists of three prime components viz. a positive electrode (cathode), a negative electrode (anode), a separator, as shown in Figure 1a.[1] All three components have porous structures, where the pores are filled with a liquid electrolyte. The liquid electrolyte acts as a medium for Li-ion transfer between the electrodes during the battery operation.

a) b)

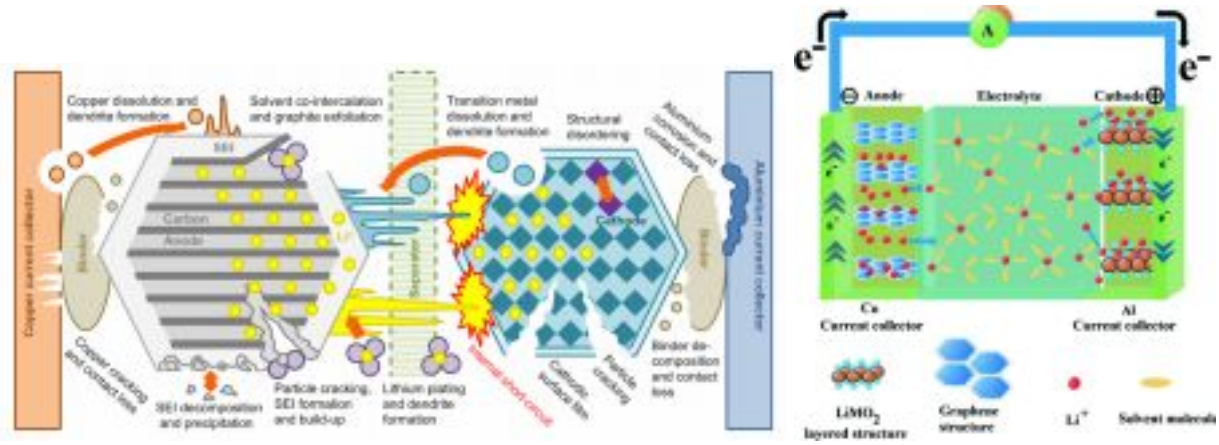

Figure 1. a) Schematic of a Li-ion battery.[1] b) Schematic of various degradation mechanisms in a Li-ion battery based on liquid electrolytes.[2]

Despite the widespread use of the liquid-electrolyte based Li-ion batteries, they suffer from several degradation mechanisms and severe safety challenges, as shown in Figure 1b.[2] Most of the liquid electrolytes used in the Li-ion batteries are solutions of Li salts in organic solvents such as ethylene carbonate, dimethyl carbonate, diethyl carbonate, etc. Such solvents are electrochemically unstable below 1V vs. Li/Li-ion, which is the operating potential range of most widely used carbon-based anodes (hard carbon, graphite, etc.).[3] This causes the electrolyte to reduce on the anode surface and form an insoluble, ionically conducting layer known as a solid electrolyte interface (SEI). The reduction of the electrolyte leads to loss of the Li inventory of the battery, and consequently its capacity. Over the lifetime of a battery, this SEI layer continues on growing to cause the battery to degrade. SEI-led degradation is even more severe when Li metal is used as an anode.[3] Secondly, the solvated Li-ions co-intercalate into the active material particles of the carbon-based anodes, which cause the exfoliation of the graphene layers and loss of the active material.[3] Lastly, Li-ions are known to deposit in metallic form and form hair-like structures called dendrites on the surface of the carbon-based anode, especially

graphite, and Li
anode under low temperature or high current operations. The dendrites can penetrate the porous separator and get in contact with the cathode, thereby causing an internal short-circuit, as shown in Figure 1b. Moreover, the organic solvents used in liquid electrolytes are highly flammable, thus making the Li-ion battery based on them highly susceptible to catching fire.

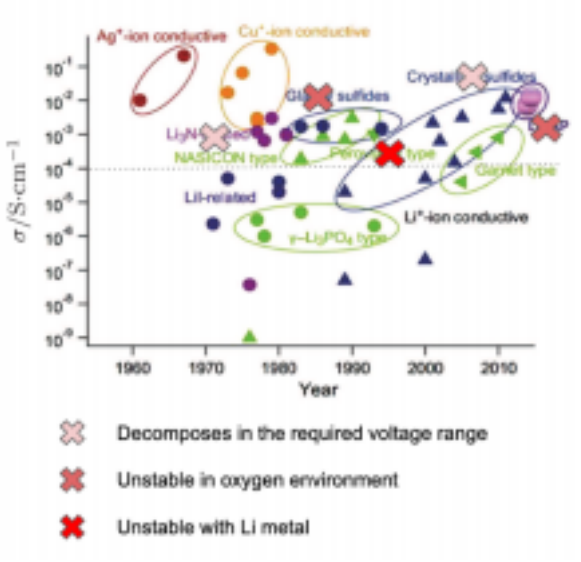

Since most of the aforementioned issues are associated with the organic solvents and the liquid state of the electrolyte, they can be overcome by replacing the liquid electrolyte with solid-state electrolytes. Additionally, solid-state electrolytes facilitate the design of Li-ion batteries with much higher energy density as they enable pack miniaturization, use of high voltage cathode materials, Li-metal anode, and Sulfur cathodes.[4]

Despite the apparent benefits, the solid-state batteries are far from commercialization as the discovery of solid-state Li-ion conductors has been slow. The discovery of new Li-ion conductors has primarily progressed by extending the already known superconducting compounds into new compositional spaces, that too experimentally. Figure 3 shows the history of the discovery of the different solid state conductors between 1960 and 2010.[4] It can be seen that only ten classes of Li-ion conducting materials have been discovered from over five decades of research. Furthermore, when the know Li-ion conducting material classes are evaluated on the following design requirements for battery application: a)[3]. high Li-ion conductivity (> 1e-4 S/cm) at room temperature, b) stability in wide voltage range against Li/Li-ion (0-5.5 V), c) inertness towards Li metal, d) inertness towards oxygen

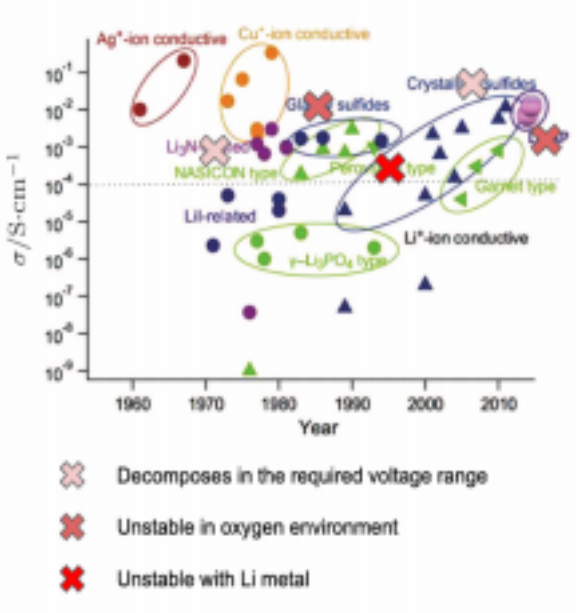

Figure History of the discovery of the solid-state Li-ion conductor. The crosses represent the non-fulfillment of one of the design criteria.[4]

environment[4], we are only left with a handful of options as shown in Figure 4.[4] It is this slow pace of the discovery of Li-ion conductors that calls for a need for an overhaul of the current discovery approach and application of an integrated MGI approach that combines the powerful yet independently used methods of data-led knowledge discovery, and estimation of the required properties through computation and experiments. The material science community has already made some efforts in this direction. In this document, we will first summarize the efforts made so far along with providing a critique on the utility of the integrated approaches used so far. Secondly, we will propose an MGI approach that can overcome some of the limitations of the methods
reported in the literature so far.

Review of the approaches reported in the literature and preliminary results:
1. Unsupervised clustering of XRD data:

The lack of large database for Li-ion conductivity values hinders any data-led knowledge discovery pertaining to the structure-conductivity relations. Though some studies which use employ linear regression models for correlating the known conductivity values with the structural features such as an average number of Li-Li bonds, Li-Li and Li-anion bond lengths, sublattice coordination etc.[5] However, the employed method is highly susceptible to overfitting as only 40 data points were used for fitting the model. Secondly, Li diffusivity (thereby, conductivity) is a tensor of rank 3, which cannot be correlated with the scalar quantities used in the study.

Unsupervised machine learning is a great method for circumventing the problem with the lack of labeled data, and XRD data makes a good dataset for performing the unsupervised clustering as we have an abundance of the XRD data and it has direct information about the structure of a material, even though convoluted. Zhang and coworkers reported the use of unsupervised clustering of the XRD data for discovering new good Li-ion conductors.[6] We adopted their approach for top-down spectral clustering of the anion sublattice in this work. We employed hierarchal clustering on ternary and quaternary Li and O containing compounds. We obtained ~15,000 XRD patterns from MP. In the first step of hierarchical clustering, we decided to find similarities and differences between potential materials based on crystal structures.

The clustering algorithm we used for hierarchical clustering is called the Uniform Manifold Approximation and Projection (UMAP). It is a non-linear dimensionality reduction approach. We looked at all the XRD data as a spectrum, and firstly we analyzed the occurrence of peaks in all the XRD patterns. The first step of our clustering resulted in two distinguished clusters, as shown in Figure 4a. The compounds in the cluster on the right side have low structural as most of them have triclinic, monoclinic structures. In comparison, compounds in the left clusters have high symmetry crystal structure such as cubic, hexagonal. Although, the demarcation is not perfect as compounds with an orthorhombic crystal structure are present in both the clusters. Therefore, we
need further refinement of our clustering. Thus, for making the analysis more accurate, we

considered the intensity for each of those clusters to differentiate the XRD patterns based on their composition and assigned the real intensity value of the spectrum. The second level of clustering resulted in several smaller clusters, as shown in Figures 4b and 4c.

The distinct clusters achieved based on XRD data shows the efficacy of the deployed method to group the compounds with similar structure together. For further refinement of the clusters, we need more material descriptors. We describe the different material descriptors we selected in the following sections.

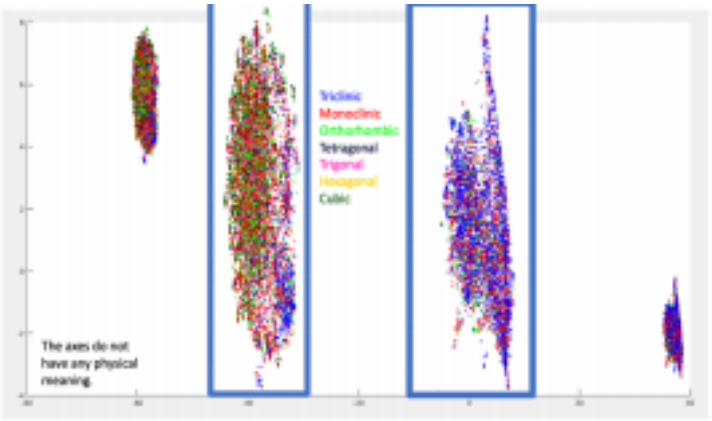

a)

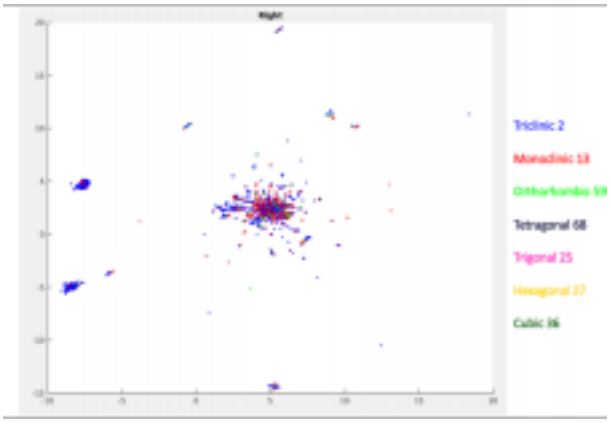

b)

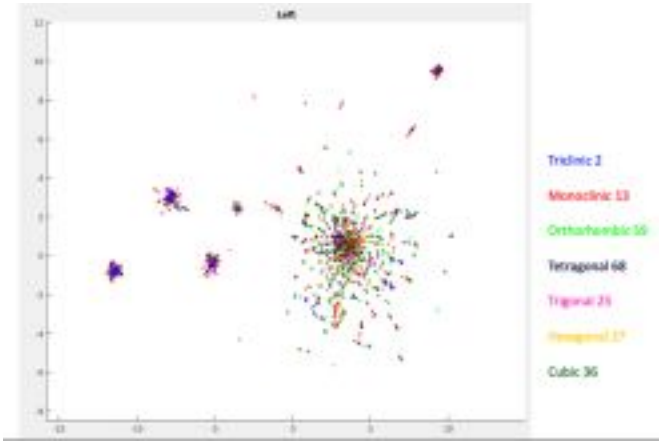

c)

Figure 4. a) The two clusters achieved by the first level of unsupervised clustering of the XRD data. Further split of the two clusters are shown in b) and c).

2. Anion sublattice:

In their work[7], Wang and coworkers identified an essential structure-property relation for predicting good Li-ion conductors. They reported that the Li containing crystalline materials where the anion forms a BCC sublattice are good Li-ion conductors. We tested their finding by analyzing the anion sublattice of materials (with high Li-ion conductivity, > 1e-5 S/cm) in the list curated by us. We used the structure matcher function with a framework comparator in the Pymatgen library[8]
for testing the match between the anion sublattice and a standard bcc structure (Fe, mp-13, at room temperature). Table 1 summarizes our findings, along with the actual anion sublattice structure from the literature. It can be seen that the results of the structure matcher function are pretty accurate. However, it is interesting to observe that not all the compounds with high Li-ion conductivity have a BCC anionic sublattice, e.g., Li_2SnS_3, which has a room temperature conductivity value of 1e-4 S/cm, has an FCC anionic sublattice[9]. Therefore, the criterion of a BCC anionic sublattice does not apply to all the materials, and we need to identify and incorporate additional material features that can explain the conductivity data trend for a more diverse set of materials.

Table 1. Comparison of the anion sublattice predicted by the structure matcher and reported in the literature.

Compound	**Anion sublattice match with BCC using structure matcher**	**Actual anion sublattice structure**
Li_3PS_4	TRUE	BCC[7]
Li_2SnS_3	FALSE	FCC[9]
$LiLaTi_2O_6$	FALSE	Not BCC
Li_3N	FALSE	HCP[10]
Li_3BrO	TRUE	BCC[11]
$Li_7P_3S_{11}$	TRUE	BCC[7]
Li_3InCl_6	FALSE	CCP
$Li_{10}Sn(PS_6)_2$	TRUE	BCC[7]
$Li_{10}Ge(PS_6)_2$	TRUE	BCC[7]
$Li_{10}Si(PS_6)_2$	TRUE	BCC[7]
Li_3P	FALSE	HCP[10]
$Li_7La_3Zr_2O_{12}$	FALSE	Not BCC

Li_6PS_5Cl	FALSE	Not BCC[7]

3. Electronic and phonon band structures as additional material features:

From the literature[5,6,12], we have curated a dataset of 128 Li containing crystalline compounds whose conductivity is known either from experimental or ab initio methods. These compounds have been into four classes: groups I, V, VI, and VII of the periodic table. Li conductivity can be expressed as $\sigma = \sigma_0 \exp(-E_a/kT)$. Figure 5a. shows the RT Li conductivity σ plotted against the activation barrier E_a for 108 of the 128 compounds, which are listed in Materials Project (MP).[13] The linear trend observed over 14 orders of conductivity suggests that the pre-factor σ_0 is roughly constant for all the materials, and E_a is critical in determining σ. We hypothesize that the average vibrational frequency for Li atoms is not significantly different across all compounds. The activation barrier E_a is related to the local bonding environment of the Li atoms.

The following section describes a few case studies and trends observed in our conductivity dataset (108 compounds), following which we propose to investigate electronic and phononic band structures in greater detail. From our dataset, we were able to compare the activation barriers/ionic conductivity for compounds having identical crystal structures and elemental compositions, only differing in the anion species. As an example, Figure shows that the activation barriers of Li_4GeO_4, Li_4SiO_4, Li_3PO_4, and Li_3N were decreased (and RT conductivity increased) by substituting the anions with S, S, S, and P respectively.

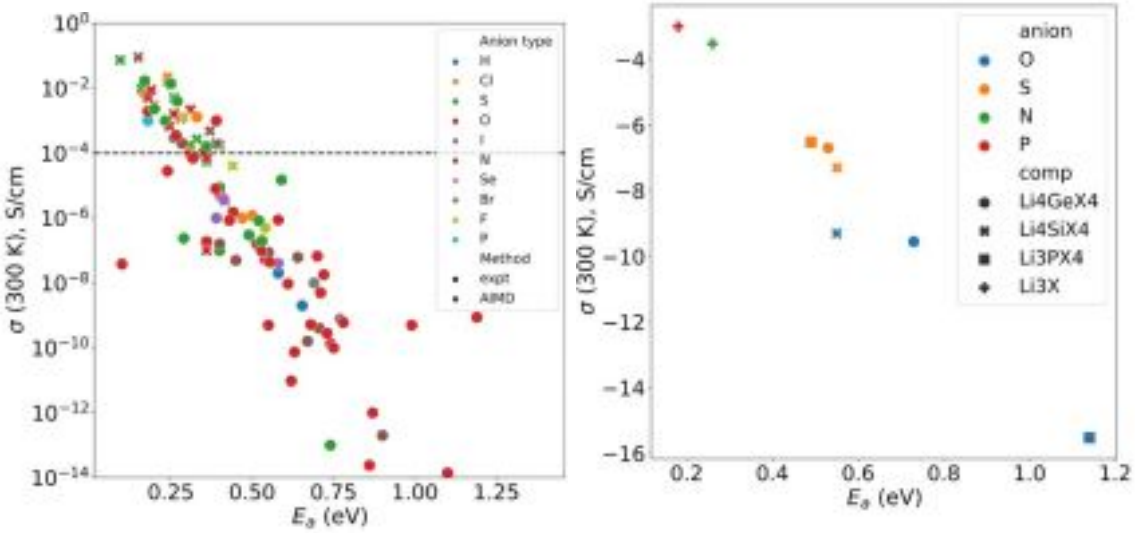

Figure 5. a) Linear behavior of σ(300K) vs. E_a indicates that σ_0 is approximately uniform, and E_a is the critical parameter. The dashed line at σ(300K) = 1E-4 S/cm shows the commonly considered criterion for superionic behavior. b) The substitution of anion species with a heavier element in the same group reduces the activation barrier and increases the RT ionic conductivity. b) The average thermal energy of neutrons at room temperature (300 K) is given by kT = 25 meV. For two Li conducting materials differing by only the anionic species, the materials with the heavier anion will have a lower average phonon band

center, favoring the activation of certain phonon modes at room temperature.

For the materials in our dataset, simple scalar quantities such as sub-lattice electronegativity, nearest neighbor count, bond length, etc. were not found to correlate with conductivity or the activation barrier. Hence, we explored parameters in the reciprocal space, which can be presumed to describe conduction better. In general, in Li contains compounds, the lighter Li atoms contribute more to the high-frequency optical modes. Heavier atoms like the anion species and other d-block or f-block elements contribute to the low-frequency acoustic modes. One important descriptor to characterize phonon band structures is the phonon band center, which can be evaluated over the element resolved or cumulative density of states.

$$\omega_{av} = \frac{\int \omega \mathrm{DOS}(\omega) d\omega}{\int \mathrm{DOS}(\omega) d\omega}$$

Due to the scarcity of existing phonon dispersion data for the compounds depicted in Figure 6a. (phonon dispersions are available for only 13 compounds)We decided to investigate other Li containing compounds as well. From MP, we identified 134 Li containing materials with published electronic and phononic band structures (no other elemental/structure restrictions imposed). In other words, these 134 compounds can have other p,d,f block elements as constituents, which were commonly observed in the conductivity database that we have curated. In Figure 6a, we present the computed Li phonon band centers, classified according to 3 metrics: crystal structure, anion chemistry, and the total number of elements. The lack of any correlation suggests that Li projected vibrational frequencies do not play a crucial role in influencing conductivity. The mean
Li project phonon band center energy is scattered in a small window centered around 41 meV. To investigate further, we computed the total phonon band centers, integrated over all atoms in the compound. The total phonon band center can influence activation barriers since heavier elements in the compound will lower the band center energy, closer to the mean thermal energy of 25 meV at RT.

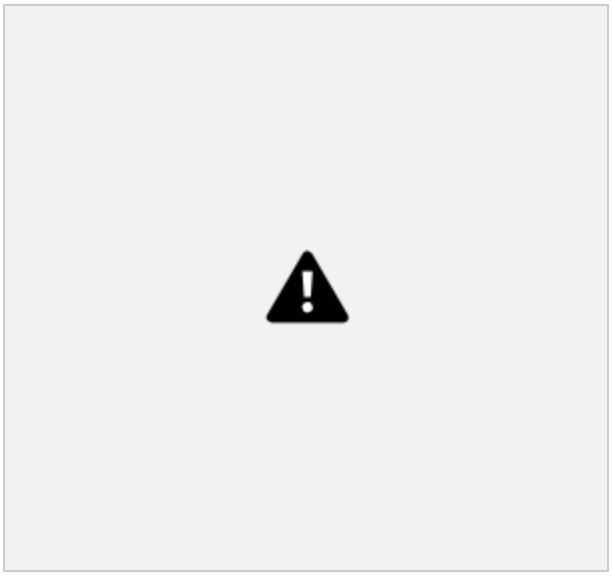

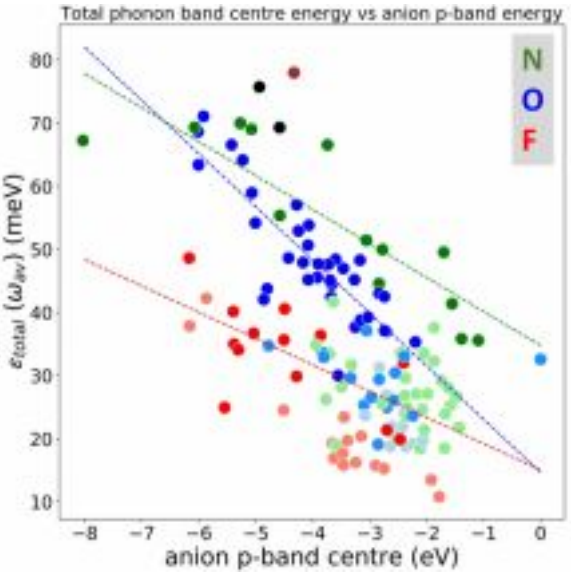

Figure 6. a) Across all crystal structures, anions species and composition space, the element resolved phonon band center for Li is found to vary in a small window centered around 41 meV. 2 compounds were found to have $\varepsilon(\omega_{av})$< 35 meV and are not shown in the scatter plot. b). Negative correlations between the average phonon band center energy and anion p-band energy referenced to the middle of the bandgap. Dashed lines depict linear trends observed for N, O, and F compounds. Lighter hues represent anions belonging to that particular periodic table group. Black and brown scatter points represent H and C,
respectively. Due to limited phonon calculations available for crystals with known conductivity, MP was screened to identify materials with both electronic band structure and phonon band structure entries.

Recent literature[14] reports indicate a positive correlation between the total phonon band center and the migration barrier for diffusion. Increasing Se content in $Na_3PS_{4-x}Se_x$ was shown to reduce the migration barrier for Li diffusion (and increase the conductivity), consistent with trends discussed earlier. Increasing Se content also reduces the total phonon band center energy since Se is heavier than S. In another article[15], the barrier for O migration in perovskites was shown to bear negative correlations with the electronic band center of the O p-bands. Following the ideas discussed in the literature, we examined correlations between electron and phonon dispersion spectra in our 134-compound dataset.

For a given compound, the element with the largest electronegativity value was designated as the anion species. The p-band center was computed by integrating the density of all the occupied electronic states and referenced with respect to the center of the bandgap. As expected, the Li phonon centers did not show any trend. The total phonon dispersion shows a negative correlation with the anion p-band center. In Figure 6b., we plot the total phonon band center against the anion
p-band centers. The dashed lines showed the linear trend observed for compounds with N, O, and F as the anions. Other scatter plots with lighter hues represent anions in the corresponding group in the periodic table. Green hues are for pnictogenides, blue for chalcogenides, and red for halides. Black and brown scatter points represent H and C, respectively. It is noted from the Figure 6b. that for N, O, and F based compounds, the total phonon band center energy is correlated negatively with the N-p, O-p, and F-p band centers. A weaker correlation is observed for other halide-based compounds, shown in the light red scatter points. Other nitrogen family anions (P, As and Bi) are found to cluster in the bottom right region of the plot. A similar lattice dynamics based representation was recently described by Muy et al.[16]

It is re-emphasized here that data presented in Figures 6a. and 6b. are for those Li compounds in MP whose electronic and phononic dispersions have been calculated. For the 128 materials with known Li conductivity, electronic structure data exists for 89 and phonon structure data for only 13. It was hence not very meaningful to examine trends and correlations to explore underlying physics.

Proposed research:

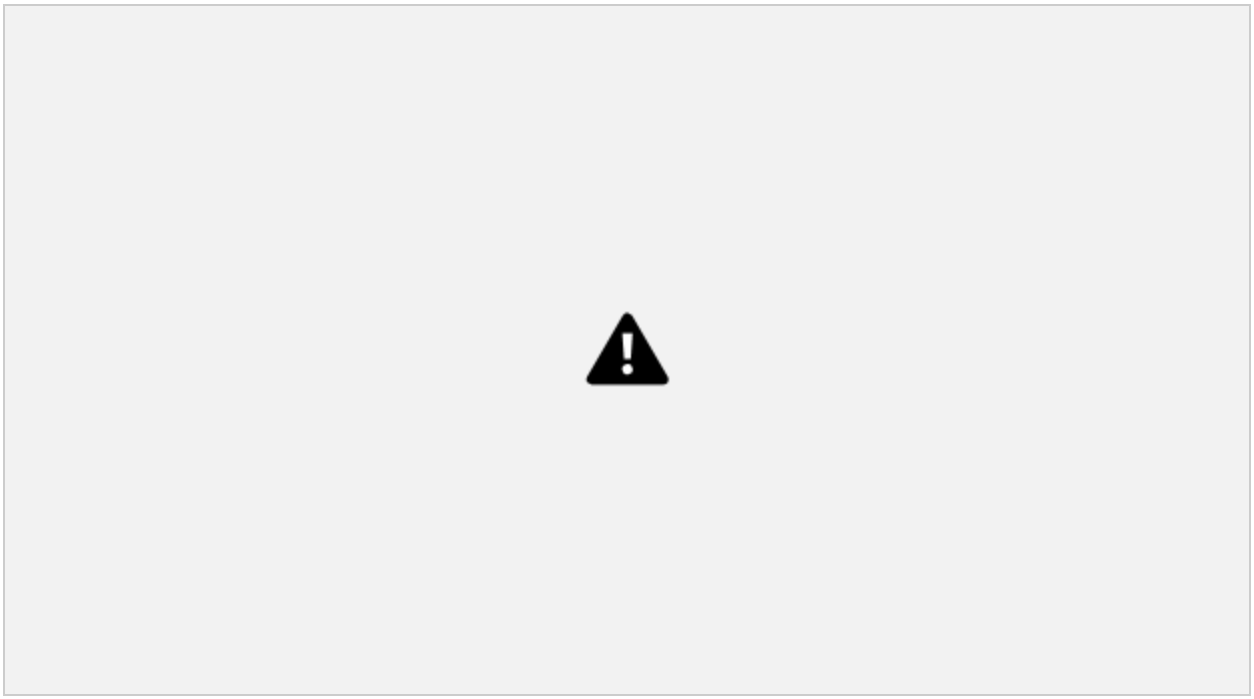

Figure 7. Flowchart indicating our proposed approach.

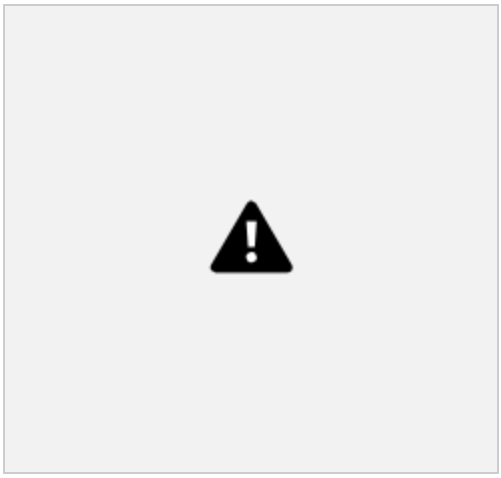

Figure 8. Anion p-band center for compounds with known conductivity.

1. Band structure screening:

Na migration barrier in the $Na_3PS_{(4-x)}Se_x$ group has been shown to correlate with the total phonon band center. Separately, oxygen band centers in a class of perovskites have been shown to correlate with oxygen migration barriers. The preliminary data indicates a relation between the total phonon band center and anion band center for several compounds. However, computing any linear relationship of the band structure properties with experimental data requires additional caution. For simple isostructural compounds with different chemistries, migration barriers are related to the band structure. Since Li conductors are known to have up

to 6 elements and are stable in several polymorphs, a direct comparison with experimentally measured activation energy is not entirely accurate. It is necessary to separate the formation and kinetic migration barriers.

A. Electron dispersion:

Since electronic structure data for many materials have been computed by high throughput methods, it serves as our first screening level. Initially, electronic structure data will be analyzed for compounds with known ionic conductivity. Oxides, sulfides, and nitrides look promising, with many high conductivity compounds having their p-band center
around -4 eV to -3 eV from the bandgap center (refer to Figure 8). We plan to identify connections between compounds identified from XRD clustering methods and their electronic structure. Preliminary data presented here show several materials with anion p band centers around -3 eV from the bandgap center (the bottom right region in figure 7b.) These materials will be selected for the next level of computational analysis. Materials in this region also have comparatively small phonon band center energies, which has been shown in the literature to correlate with small migration barriers.

B. Phonon dispersion:

Phonon dispersion properties for materials screened in part A will be computed to narrow our material space further. Crystals with average phonon energy around 20-40 meV (room temperature vibrations) will be screened for AIMD simulations.

2. Ab initio Molecular Dynamics (AIMD) simulations:

Data generated by molecular dynamics simulations will be used to validate the developed hypotheses and also be used to refine the screening criteria. We acknowledge that AIMD simulations at 300 K are costly. Extrapolation from higher temperatures often results in larger error windows for the predicted values. Hence, it is essential to devise effective screening strategies. Once enough representative AIMD simulations are run, we plan to quantify the correlations between features and conductivity for different groups in the periodic table. We then want to realize a scheme where the electron and phonon band structures can be used as descriptors to rapidly screen and identify new materials for AIMD simulations and recommendations for experimental validation.

3. Experimental validation

The experimental validation of the predicted material is essential for validating our overall approach. If the predicted materials cannot be synthesized with the existing methods, then new processes will be developed and optimized. The phase purity will be tested using the existing techniques of XRD, SEM-EDS, TEM, ICP-AES, etc. The conductivity measurements will be conducted by performing EIS. The feedback from the experimental study will inform the previous steps, e.g., the effect of impurity, grain boundaries, etc. on the conductivity value.

Other considerations

Li compounds can also have other d and f block elements which affect the bonding characteristics. The total phonon band structure characterizes their vibrational effects. Improving the accuracy of our screening criteria requires a further understanding of this composition space. Integrating SSE materials in a battery module also requires that the SSE is stable against the electrodes under operational voltages, lattice-matched to avoid large strains, etc. These considerations will also be accounted for in our materials selection procedure.

Impact of the proposed work

Our proposed approach attempts at overcoming the limitations of various methods reported in the literature for bridging the information gap that exists between the data and computation. We combine the unsupervised clustering of the XRD data, with the anion sublattice, electronic and phononic band structures as the critical descriptors for predicting the conductivity of multiple classes of Li-ion conducting materials. The most important contribution that can arise from our study is the correlation between the electronic and phononic band structures, screening criteria for various classes of materials based on these structures. Additionally, the experimental study can contribute new synthesis methods to the literature. Lastly, the success of this study will be another step forward in the use of the MGI approach for discovering solid-state electrolyte materials for Li-ion batteries.

References:

1. Dutta, P. K. *et al. Nano-/Micro-engineering for Future Li-Ion Batteries*. (Springer Singapore, 2019). doi:10.1007/978-981-13-3269-2_7
2. Birkl, C. R., Roberts, M. R., McTurk, E., Bruce, P. G. & Howey, D. A. Degradation diagnostics for lithium ion cells. *J. Power Sources* **341**, 373–386 (2017).
3. Aurbach, D., Zinigrad, E., Cohen, Y. & Teller, H. A short review of failure mechanisms of lithium metal and lithiaded graphite anodes in liquid electrolyte solutions. *Solid State Ionics* **148**, 405–416 (2002).
4. Gao, J., Zhao, Y. S., Shi, S. Q. & Li, H. Lithium-ion transport in inorganic solid state electrolyte. *Chinese Phys. B* **25**, (2015).
5. Sendek, A. D. *et al.* Holistic computational structure screening of more than 12 000 candidates for solid lithium-ion conductor materials. *Energy Environ. Sci.* **10**, 306–320 (2017).
6. Zhang, Y. *et al.* Unsupervised discovery of solid-state lithium ion conductors. *Nat. Commun.* **10**, 1–7 (2019).
7. Wang, Y. *et al.* Design principles for solid-state lithium superionic conductors. *Nat. Mater.* **14**, 1026–1031 (2015).
8. Ong, S. P. *et al.* Python Materials Genomics (pymatgen): A robust, open-source python library for materials analysis. *Comput. Mater. Sci.* **68**, 314–319 (2013).
9. Brant, J. A. *et al.* Fast lithium ion conduction in Li2SnS3: Synthesis, Physicochemical characterization, and electronic structure. *Chem. Mater.* **27**, 189–196 (2015). 10. Materials project (https://materialsproject.org/).

11. Emly, A., Kioupakis, E. & Van Der Ven, A. Phase stability and transport mechanisms in antiperovskite Li3OCl and Li3OBr superionic conductors. *Chem. Mater.* **25**, 4663–4670 (2013).
12. Sendek, A. D. *et al.* Machine Learning-Assisted Discovery of Solid Li-Ion Conducting Materials. *Chem. Mater.* **31**, 342–352 (2019).
13. Jain, A. *et al.* Commentary: The materials project: A materials genome approach to accelerating materials innovation. *APL Mater.* **1**, (2013).
14. Krauskopf, T. *et al.* Comparing the Descriptors for Investigating the Influence of Lattice Dynamics on Ionic Transport Using the Superionic Conductor Na3PS4-xSex. *J. Am. Chem. Soc.* **140**, 14464–14473 (2018).
15. Mayeshiba, T. T. & Morgan, D. D. Factors controlling oxygen migration barriers in perovskites. *Solid State Ionics* **296**, 71–77 (2016).
16. Muy, S. *et al.* High-Throughput Screening of Solid-State Li-Ion Conductors Using Lattice Dynamics Descriptors. *iScience* **16**, 270–282 (2019).

Supplementary information

Budget:

The project will be headed by 2 PI's, one computational scientist and one experimentalist. 2 Ph.D. students will work on this project.

Year I		**Year total**
Professor salaries	$100,000	
Ph.D. student salaries	$75,000	
Computing	$65,000	$240,000
Year II		
Professor	$100,00	
Ph.D. student salaries	$75,000	
Computing	$43,000	
Experiment	$25,000	
Material	$15,000	$258,000
Year III		
Professor salaries	$100,000	
Ph.D. student salaries	$75,000	
Material	$35,000	

Equipment	$75,000	$285,000
Travel + miscellaneous	$17,000	
TOTAL AMOUNT REQUESTED		**$800,000**

Data management and dissemination:

All computational and experimental data generated from our work will be hosted in a freely accessible repository. Materials data will be appended to MP, where applicable. The relevant machine learning algorithms and codes will be available on GitHub, for download and modification.
The following types of data will be generated and recorded:

1. Electron and phonon dispersions
2. Diffusivity, conductivity and activation barriers categorized by crystal and element type
3. Experimental synthesis maps
4. XRD patterns, micrographs, spectroscopy data.